ENDOR and Special TRIPLE Resonance Spectroscopy of Photoaccumulated Semiquinone Electron Acceptors in the Reaction Centers of Green Sulfur Bacteria and Heliobacteria†

Irine P. Muhiuddin,‡ Stephen E. J. Rigby,‡ Michael C. W. Evans,§ Jan Amesz,|| and Peter Heathcote*,‡

School of Biological Sciences, Queen Mary and Westfield College, University of London, Mile End Road, London E1 4NS, U.K., Department of Biology, University College London, University of London, Gower Street, London WC1E 6BT, U.K., and Department of Biophysics, Huygens Laboratory, University of Leiden, P.O. Box 9504, 2300 RA Leiden, The Netherlands

Received August 24, 1998; Revised Manuscript Received March 2, 1999

ABSTRACT: Photoaccumulation at 205 K in the presence of dithionite produces EPR signals in anaerobically prepared membranes from *Chlorobium limicola* and *Heliobacterium chlorum* that resemble the EPR spectrum of phyllosemiquinone ($A_1^{\bullet-}$) photoaccumulated in photosystem I. We have used ENDOR and special TRIPLE resonance spectroscopy to demonstrate conclusively that these signals arise from menasemiquinone electron acceptors reduced by photoaccumulation. Hyperfine couplings to two protons H-bonded to the semiquinone oxygens have been identified by exchange of *H. chlorum* into D_2O, and hyperfine couplings to the methyl group, and the methylene group of the phytyl side chain, of the semiquinone have also been assigned. The electronic structure of these menasemiquinones in these reaction centers is very similar to that of phyllosemiquinone in PSI, and shows a distorted electron spin density distribution relative to that of phyllosemiquinone in vitro. Special TRIPLE resonance spectrometry has been used to investigate the effect of detergents and oxygen on membranes of *C. limicola.* Triton X-100 and oxygen affect the menaquinone binding site, but *n*-dodecyl β-D-maltoside preparations exhibit a relatively unaltered special TRIPLE spectrum for the photoaccumulated menasemiquinone.

The green sulfur bacteria and heliobacteria are strictly anaerobic photosynthetic organisms with oxygen-sensitive reaction centers which has made their study difficult. However, progress in characterizing their reaction centers has accelerated in recent years with improved preparations, particularly for the reaction center of green sulfur bacteria (*1*, *2*).

Both bacteria possess reaction centers that resemble photosystem I (PSI)[1] of oxygenic photosynthesis (*3*−*6*). These reaction centers are classified as type I (*7*) or ferredoxin-reducing reaction centers. The electron transfer chain begins with the primary electron donor, comprised of a bacteriochlorophyll *a* (BChl *a*) pair (*8*, *9*) in the reaction center of green sulfur bacteria termed P840. Bacteriochlorophyll *g* (BChl *g*) acts as the primary electron donor, probably as a dimer known as P798, in the reaction centers of heliobacteria.

From the primary electron donor, the electron is transferred to the primary electron acceptor, A_0. This is a monomeric chlorophyll *a*-like molecule (*11*, *65*) in green sulfur bacteria, while in heliobacteria, it is thought to be 8^1-hydroxychlorophyll *a* (*10*). The remaining electron acceptor molecules include iron sulfur centers starting with center F_X as in PSI. From the latter, the electron is transferred to the terminal electron acceptors F_A and F_B that in the green sulfur bacteria are located on a membrane extrinsic protein subunit resembling the PsaC subunit present in PSI (*12*, *13*).

All three of these iron sulfur centers have been detected using EPR in the reaction center of green sulfur bacteria (*14*). In the reaction center of heliobacteria, EPR evidence for center F_X is still lacking (*15*). However, it is thought to exist since the region thought to bind center F_X in PSI and in the reaction center of green sulfur bacteria is highly conserved in heliobacteria (*16*).

The components of the electron transfer chain up to F_X are located in the membrane-spanning domain of the reaction center. In both green sulfur bacteria and heliobacteria, this is thought to consist of two identical polypeptide subunits that are bridged by the two chlorophyll molecules that comprise the primary electron donor and center F_X. This homodimeric arrangement is unlike the situation encountered in other photosystems studied so far, where the reaction center core is composed of a heterodimer of proteins. Evidence for this homodimeric arrangement was initially provided by genetic studies, where only a single gene

† This work was supported by a grant from the U.K. Biotechnology and Biological Sciences Research Council (BBSRC) (CO 6041) and the award of a BBSRC postgraduate research studentship to I.P.M. J.A. was supported by the European Union (Contract FMRX-CT96-0081).

* To whom correspondence should be addressed.

‡ Queen Mary and Westfield College, University of London.

§ University College London, University of London.

|| University of Leiden.

[1] Abbreviations: ENDOR, electron nuclear double resonance; EPR, electron paramagnetic resonance; ESP, electron spin-polarized; PSI, photosystem I; P700, primary electron donor of photosystem I; P840, primary electron donor in green sulfur bacteria; P798, primary electron donor in heliobacteria; A_o, chlorophyll primary electron acceptor in photosystem I; A_1, phylloquinone secondary electron acceptor in photosystem I; F_A, F_B, and F_X, [4Fe-4S] centers of photosystem I; BChl, bacteriochlorophyll; PhQ, phylloquinone; MQ, menaquinone; FMN, flavin mononucleotide; DM, *n*-dodecyl β-D-maltoside; hfcs, hyperfine couplings; RC, reaction center.

10.1021/bi982042u CCC: $18.00
Published on Web 05/13/1999

resembling *psaA* and *psaB* that encode the reaction center core polypeptides of PSI was identified (*12*, *16*, *17*).

Conclusive evidence for the participation of a quinone electron acceptor functioning between A_0 and F_X in these bacterial type I reaction centers is still lacking. Such an acceptor termed A_1 has been shown to function in PSI (*18*−*20*). There it is a phylloquinone (PhQ) molecule also known as vitamin K_1. For many years, there was considerable controversy concerning the nature and role of such an electron acceptor in PSI (see ref *21* for a recent review). Similar controversies now apply to the reaction centers of green sulfur bacteria and heliobacteria (*3*−*6*).

Quinone species have been identified in both heliobacteria and green sulfur bacteria that could perform the role of a secondary electron acceptor equivalent to the A_1 PhQ acceptor found in PSI. Menaquinones (MQs) are a family of quinone compounds that are closely related to PhQ. Of this family, MQ-7−10 (that differ in the number of isoprene chain units attached to the quinone head) have been identified as the only quinones in heliobacteria (*22*). Only MQ-7 has been identified in the green sulfur bacteria (*23*), in addition to the *Chlorobium* quinone and 1′-hydroxymenaquinone-7 that have also been shown to be present (*23*).

The presence of a semiquinone electron acceptor in heliobacteria and green sulfur bacteria was suggested (*24*, *25*) by the observation of high-*g* value EPR radical signals that photoaccumulated during freezing (see below). Charge recombination kinetics in heliobacteria at low temperatures compared to those observed in PSI appeared to be faster than might be expected for the recombination of $P798^+F_X^-$ but slower than expected for $P798^+A_o^-$ (*15*, *26*). The long-lived photobleaching (0.6 ms) of P798 was dependent on a two-electron reduction during redox titration (*27*), possibly indicating double reduction of a quinone electron acceptor. Nitschke et al. (*14*, *67*) reported that dark reduction with dithionite of a sample from green sulfur bacteria, followed by photoaccumulation of the reduced iron sulfur centers, maximized the yield of the triplet of P840, again suggesting double reduction of a quinone.

However, removal of MQ from membranes of heliobacteria has been found to have no effect on electron transfer within the reaction center (*28*). Reaction center preparations were isolated from green sulfur bacteria that retained photochemical activity even though they did not contain menaquinone (*29*, *30*). The reoxidation of A_o in bacterial type I reaction centers apparently occurs around 600 ps in green sulfur bacteria (*31*) and heliobacteria (*32*, *33*), i.e., much slower than the 20−30 ps phase reported for the reoxidation of A_o in PSI (*34*−*36*). Lin et al. (*37*) reported that the only charge-separated state observed after $P798^+A_o^-$ in *Heliobacillus mobilis* by picosecond difference absorbance spectroscopy above 400 nm was $P978^+F_X^-$. Brettel et al. (*38*) have recently reported that spectroscopic measurements of *Hc. mobilis* membrane fragments between 360 and 450 nm provide no evidence for reduction of menaquinone between 2 ns and 4 μs after a flash. Photovoltaic measurements (*38*) indicated that A_o was reoxidized with a single kinetic phase of 700 ps, and the relative amplitude of this phase suggested that it reflected electron transfer from A_o^- to F_X. Although electron spin-polarized (ESP) signals have been reported for green sulfur bacteria (*39*, *40*), these signals appear to contain a P^+ contribution only and lack the high-field contribution from the semiquinone seen in the corresponding ESP signals arising from $P700^+A_1^{\bullet-}$ in PSI.

Conflicting results have been reported regarding the assignment to the secondary electron acceptor $A_1^{\bullet-}$ of PSI of an asymmetric EPR signal at $g \cong 2.00$ that photoaccumulated at low temperatures (200 K) under reducing conditions (*41*), or produced by illumination while freezing in the presence of reductants (*42*). However, recent evidence (*43*) shows that, in contrast to the observations of Barry et al. (*44*), line narrowing of this signal occurs upon biosynthetic deuteration of PhQ, demonstrating that the photoaccumulated signal does arise from the phyllosemiquinone $A_1^{\bullet-}$. Additional evidence for the assignment of the asymmetric EPR signal to the photoaccumulated $A_1^{\bullet-}$ acceptor came from ENDOR and special TRIPLE studies (*45*) which also yielded information about the electronic structure of this phyllosemiquinone.

As described above, photoaccumulation experiments have also been performed on the reaction centers of green sulfur bacteria (*25*) and heliobacteria (*24*). In the former study, an asymmetric EPR signal resembling the PSI-photoaccumulated $A_1^{\bullet-}$ signal at $g = 2.00$ was photoaccumulated in reduced membranes and isolated reaction centers. Photoaccumulation was achieved by illumination of dithionite-reduced samples at pH 10.0 and 196 K. A photoaccumulated EPR signal at $g = 2.00$ was also generated in membrane samples from heliobacteria (*24*).

This paper reports a study that was carried out to determine whether these EPR signals do arise from a semiquinone electron acceptor in bacterial type I reaction centers. Asymmetric EPR signals at $g \cong 2.00$ resembling $A_1^{\bullet-}$ have been observed in anaerobically prepared membranes of *Chlorobium limicola* and *Heliobacterium chlorum* following photoaccumulation at low temperatures under reducing conditions. To conclusively assign these photoaccumulated EPR signals to semiquinone species, the magnetic resonance techniques electron nuclear double resonance (ENDOR) and special TRIPLE resonance spectroscopy were employed [the results of preliminary special TRIPLE resonance studies of the photoaccumulated signal in membranes from *C. limicola* have been previously reported (*46*)]. This demonstrated that the photoaccumulated EPR signals had arisen from a 2-methylnaphthosemiquinone species and revealed that the electronic structure of the semiquinone radical was similar to that of the phyllosemiquinone $A_1^{\bullet-}$ in the PSI reaction center (*45*).

We have also monitored using special TRIPLE resonance the effect of oxygen exposure and detergents Triton X-100 and *n*-dodecyl β-D-maltoside on the semiquinone acceptor.

MATERIALS AND METHODS

Cells of *C. limicola* (strain Tassajara) were grown as described by Bratt et al. (*47*) in the presence of acetylene to inhibit bacteriochlorophyll *c* biosynthesis. Cells of *H. chlorum* were grown as previously described (*48*). Subsequent preparation of membrane fractions was carried out under argon with an oxygen trap utilizing Tricine and flavin mononucleotide (FMN) as described by Hager-Braun et al. (*49*). Preparation of solubilized fractions containing reaction centers from *C. limicola* using detergents was carried out under argon following previously published protocols [Triton

X-100 (*49*) and *n*-dodecyl β-D-maltoside (*50*)] with the inclusion of the Tricine−FMN oxygen trap in all buffers. EPR samples were prepared using as concentrated a preparation of solubilized reaction centers or membranes as possible. EPR samples in 20 mM Tris-Tricine buffer at pH 8.0 and 20 μM FMN were placed in 3 mm internal diameter quartz EPR tubes under argon and reduced by the addition of 0.2% w/v sodium dithionite for 30 min in the dark prior to freezing in liquid nitrogen in the dark. Photoaccumulation for 2 min at 205 K was carried out as described by Heathcote et al. (*51*). To exchange membranes of *H. chlorum* into deuterium oxide (D_2O), pelleted membranes were resuspended in a D_2O buffer and left overnight under argon at 4 °C, and then pelleted again prior to resuspension in D_2O buffer and preparation of samples. Control membrane samples from the same preparation of *H. chlorum* were treated in the same way but resuspended in H_2O buffer and checked to ensure that the ENDOR spectrum of the photoaccumulated $A_1^{\bullet-}$ acceptor was not altered by this treatment. Although care is taken to try to make sure that control samples and samples in D_2O were at the same concentration and in EPR tubes of the same size, differences in the amount of $A_1^{\bullet-}$ photoaccumulated were inevitable and observed by CW EPR. We have used the double integral of the CW EPR spectra of $A_1^{\bullet-}$ recorded under nonsaturating microwave powers to determine the relative spin concentrations of the semiquinone radicals in H_2O and D_2O samples and obtained a scaling factor to allow subtraction of D_2O from H_2O spectra.

ENDOR, ST, and EPR spectra were obtained at X-band using a Bruker ESP 300 EPR spectrometer as described by Rigby et al. (*52*, *53*). Spectra were corrected for a small baseline nonlinearity by the subtraction of off-resonance scans which were filtered for noise (standard Bruker software) to avoid reducing the spectrum signal-to-noise ratio. The experimental spectra were not filtered for noise. Acquisition conditions for specific spectra are given in the figure captions. The precision of the hfc determination, i.e., the variation in the hfc determination between these samples, was ±0.1 MHz. Spectra are presented in the first-derivative mode. The hyperfine coupling constants are measured from zero crossing points, except for $A_{||}$ features where the peak maximum or minimum is used.

RESULTS

Figure 1 shows EPR spectra in the $g = 2.00$ region produced by illumination at 205 K (for 2 min) of dithionite-treated *C. limicola* (Figure 1a) and *H. chlorum* (Figure 1b) membranes. The line widths ($\Delta H_{ptp} = 0.95$ mT) and g values (2.0046) of these signals are suggestive of the EPR spectrum of the $A_1^{\bullet-}$ phyllosemiquinone radical formed in PSI particles by the same treatment (*43*, *51*). These spectra also show, though to a lesser extent, the asymmetric line shape associated with $A_1^{\bullet-}$ having a shoulder at the low-field side of the spectrum. The line shapes of the signals in *C. limicola* and *H. chlorum* are slightly different, but this is expected since the line shape of the spectra reflects unresolved proton hyperfine couplings. Therefore, the line shapes will differ with the differences observed in the proton hfcs for the two radicals (see below and Tables 1 and 2).

The frozen solution ENDOR spectra of the radicals formed in *C. limicola* and *H. chlorum* are presented in Figure 2.

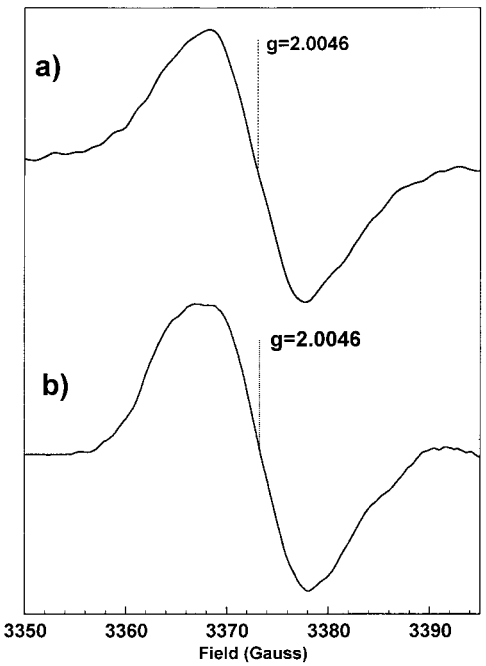

FIGURE 1: EPR spectra of the $A_1^{\bullet-}$-like radical photoaccumulated in (a) *C. limicola* membranes and (b) *H. chlorum* membranes. Both spectra were recorded in the ENDOR cavity. Conditions were as follows: microwave power of 100 μW, modulation amplitude of 1.6 G, modulation frequency of 12.5 kHz, and temperature of 120 K. Both spectra are the sums of eight scans.

Table 1: Hyperfine Coupling Constants (MHz) and Resonance Assignments for the Semiquinone Radicals of *C. limicola* and *H. chlorum* and Comparison with Those of $A_1^{\bullet-}$ of PSI (*45*)

feature	*C. limicola*	*H. chlorum*	PSI	assignment
1	3.0	3.0	3.6	3-β-CH_2 $A_\perp$
	3.8			3-β-CH_2 $A_\perp$
2	−5.4	−5.0	−5.0	H-bond $A_\perp$
	−6.2	−6.5	−5.8	H-bond $A_\perp$
3	7.5		7.6	3-β-CH_2 $A_{||}$
4	8.8	8.6	9.0	2-methyl $A_\perp$
5	11.2	10.0	13.4	H-bond $A_{||}$
6	12.3	12.2	12.8	2-methyl $A_{||}$
		13.0	13.4	H-bond $A_{||}$

Table 2: Hyperfine Coupling Constants (MHz) and Resonance Assignments for the Semiquinone Radicals of *C. limicola* in Membranes, after Extraction with Detergents, and after Exposure to Oxygen

feature	membranes	LM	TX-100	LM/O_2	assignment
1	3.0	3.4	3.6	3.0	3-β-CH_2 $A_\perp$
	3.8	3.8	4.4	3.8	
2	−5.4	−5.4	−5.8	−5.2	H-bond $A_\perp$
	−6.2	−6.2		−6.4	H-bond $A_\perp$
3	7.5	7.7	8.0	7.7	3-β-CH_2 $A_{||}$
4	8.6	8.6		8.6	2-methyl $A_\perp$

Such frozen solution ENDOR spectra of radicals taken at the EPR crossing point show all orientations of the molecules in the external field simultaneously (i.e., a powder spectrum). Features occurring in this region of the spectrum arise from protons, and the observed line shapes reflect the symmetry of the hyperfine tensors and the random orientation of the tensors in the applied field. To analyze these spectra, we will assume in the first instance that these radicals do arise from an $A_1^{\bullet-}$-like semiquinone species. The subsequent analysis will justify this assumption. As discussed in the

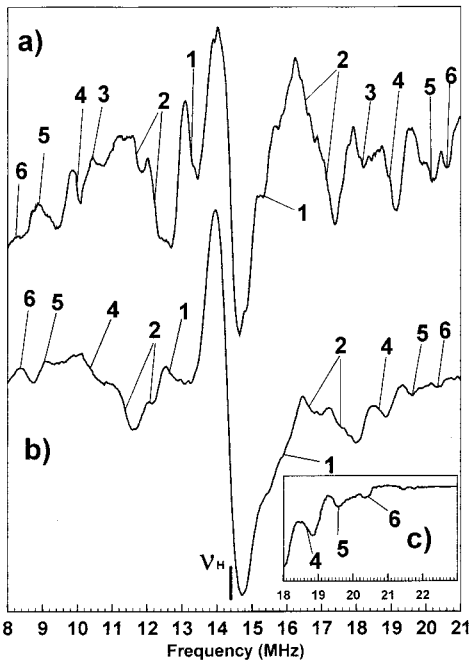

FIGURE 2: ENDOR spectra of the $A_1^{\bullet-}$-like radical photoaccumulated in (a) *C. limicola* membranes and (b) *H. chlorum* membranes. Conditions were as follows: (a) microwave power of 3.9 mW, rf power of 100 W, rf modulation depth of 199 kHz, time constant of 1310 ms, scan time of 84 s, an average of 200 scans, and temperature of 120 K and (b) the same as for spectrum a but with a microwave power of 4.9 mW, an rf modulation of 177 kHz, and a temperature of 80 K. Inset c shows part of the *H. chlorum* spectrum recorded with conditions like those described for spectrum b except the time constant was 327 ms, with an average of 360 scans.

introductory section, both *C. limicola* (*23*) and *H. chlorum* (*22*) contain menaquinones (*C. limicola* also contains 1′-hydroxy- and 1′-oxomenaquinone species) the ENDOR characteristics of which, in the semiquinone anion state, are very similar to those of the phyllosemiquinone anion radical as reported by Rigby et al. (*45*).

The most intense features of frozen solution semiquinone radical ENDOR spectra arise from the $A_\perp$ components of the axially symmetric hyperfine couplings (hfcs) to protons hydrogen bonded to the quinone oxygens (*54*) and the protons of methyl groups β to the delocalized π orbital system (*55*) bearing the unpaired electron [i.e., the singly occupied molecular orbital (SOMO)]. Features 2 and 4 in Figure 2 are particularly prominent, suggesting that they arise from either the $A_\perp$ components of the methyl group or H-bond hfcs, but these two possibilities are not distinguishable at this point. Axially symmetric hfcs each have an intense $A_\perp$ component which shows a zero crossing and a weaker $A_{||}$ turning point (*54*, *55*); therefore, features 3 (in the *C. limicola* spectrum only), 5, and 6 appear to be such $A_{||}$ components of axial hfcs. A further possible $A_\perp$ component, although less intense than features 2 and 4, is labeled as feature 1, giving a total of three axial hfcs in each spectrum each having observable $A_\perp$ and $A_{||}$ components. Feature 1 (and one of the $A_{||}$ features) probably arises from the β-CH_2 (methylene) protons of C(1′) attached at C(3) of the quinone ring (see Figure 3 for quinone structures and carbon atom numbering schemes). Such features from methylene protons have been observed in ENDOR spectra of tyrosine radicals (*52*, *56*) and semiquinone radicals (*45*, *57*). Features 5 and 6 appear rather weak especially on the high-frequency side of the *H. chlorum* spectrum (Figure 2b). To demonstrate that these features are not artifacts of the conditions used to obtain the spectra, an ENDOR spectrum was obtained using a lower time constant shown as the inset in Figure 2 (spectrum c). This spectrum confirms the existence of features 5 and 6 in the *H. chlorum* spectrum, and since it extends to 23 MHz indicates that these features are significant compared to the baseline noise level outside the frequency range of the semiquinone signals. Due to the long accumulation times that are required, it proved to be impractical to use these conditions for all spectra.

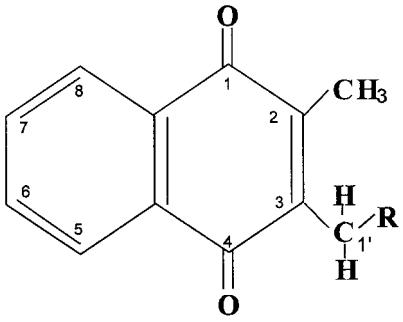

FIGURE 3: General structure of the 2-methylnaphthoquinone family of quinones with the atom numbering scheme.

Hfcs to H-bonded protons may be distinguished from those to covalently attached protons using H_2O/D_2O solvent exchange experiments. Features arising from hfcs to H-bonded protons in a spectrum recorded in H_2O will not be present in the D_2O spectrum if the protons have been exchanged for deuterons. This can be seen by simply comparing such spectra or more easily by subtracting the D_2O spectrum from the H_2O spectrum to produce a difference spectrum in which only features from exchangeable (H-bonded) protons are present. Such solvent exchange spectra are shown for the radical in membranes of *H. chlorum* in Figure 4 (see Materials and Methods for the exchange protocol). The H_2O/D_2O exchange is not complete, but is estimated to be 80% on the basis of the decrease in intensity of the exchangeable features. The difference spectrum (Figure 4c) clearly assigns features 2 and 5 to the $A_\perp$ and $A_{||}$ components, respectively, of hfcs to H-bonded protons. A further exchangeable $A_{||}$ feature, which is hidden under feature 6 in Figures 2b and 4a, is indicated by an asterisk (*). H-bond hfcs are essentially traceless (*54*), i.e., $2A_\perp - A_{||}$ (ignoring the negative sign of the $A_\perp$ component), and features 2 and 5 and the new feature denoted with an asterisk form two sets of $A_\perp$ and $A_{||}$ components which fulfill this criterion. Although the feature denoted with an asterisk is admittedly not particularly prominent on the high-frequency side of the spectrum, we believe it to be above the noise on the low-frequency side. A similar feature at the same position is seen in the ENDOR spectrum of the phyllosemiquinone radical in photosystem I (*45*), which in our opinion further strengthens the case for assigning this rather weak feature. Note that the *H. chlorum* radical shows two completely resolved H-bond hfcs, unlike $A_1^{\bullet-}$ of PSI (*45*). A further resolved exchangeable feature with an hfc of 2.0 MHz is also revealed in the difference spectrum (Figure 4c, denoted with arrows). The origin of this feature is not clear. The intensity of this feature and the magnitude of the hfc suggest that it arises from the $A_\perp$ component of a coupling to a proton

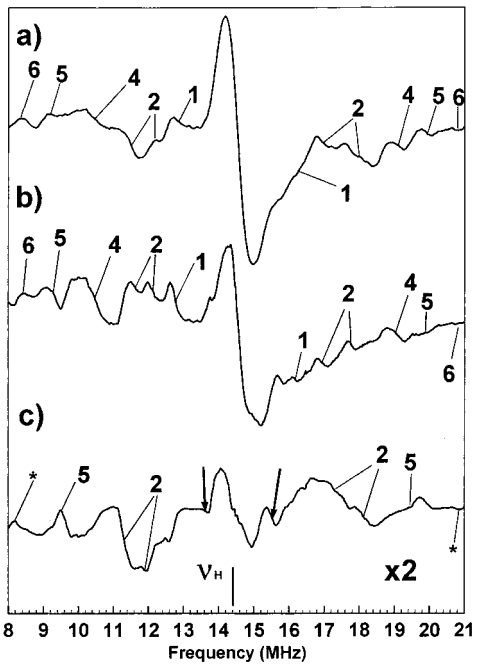

FIGURE 4: ENDOR spectra of the $A_1^{\bullet-}$-like radical photoaccumulated in *H. chlorum* membranes incubated in (a) H_2O buffer and (b) D_2O buffer. Spectrum c shows the difference spectrum of spectrum a minus spectrum b. Conditions were like those described in the legend of Figure 2b.

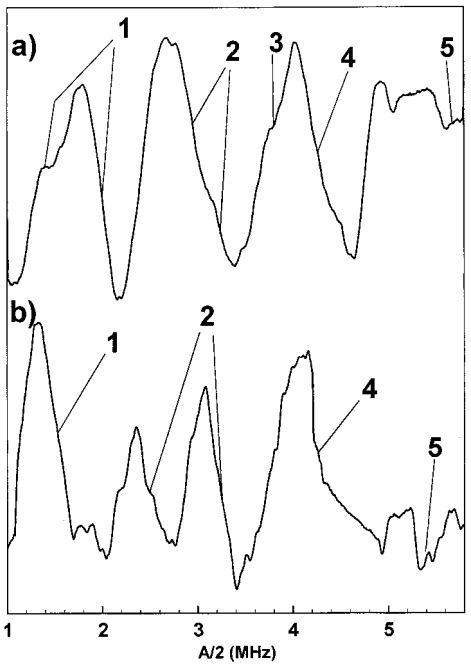

FIGURE 5: Special TRIPLE spectra of the $A_1^{\bullet-}$-like radical photoaccumulated in (a) *C. limicola* membranes and (b) *H. chlorum* membranes. Conditions were as follows: (a) microwave power of 3.9 mW, rf power of 200 W, rf modulation depth of 177 kHz, time constant of 1310 ms, scan time of 84 s, an average of 200 scans, and temperature of 120 K and (b) the same as for spectrum a but with a microwave power of 4.9 mW, a modulation depth of 158 kHz, and a temperature of 80 K.

that is significantly closer to the semiquinone than the majority of the protein protons. It may arise from a proton that forms a secondary weak H bond to a semiquinone oxygen. We were not successful in detecting H_2O/D_2O exchange in the *C. limicola* radical, probably due to access of the solvent to the reaction center being limited by the greater size and complexity of the membrane-bound pigment−protein reaction center complex in this organism. Features 2 and 5 in the *C. limicola* spectrum (Figure 2a) are therefore assigned to H-bonded protons by analogy with the *H. chlorum* radical and PSI $A_1^{\bullet-}$ and since two of the features form a traceless $A_\perp/A_{||}$ pair as described above. Such large H-bond hfcs are typical of semiquinone radicals in biological systems; ENDOR spectra of chlorophyll radicals (cation or anion) do not exhibit such features.

The assignment of the features arising from H-bonded protons above allows feature 4 to be assigned to the $A_\perp$ component of the 2-methyl group hfc. Semiquinone methyl hfcs follow the relationship $A_{||} = A_\perp + \sim 3.5$ MHz (*55*). Feature 6 fulfills this relationship in the spectra of both the *C. limicola* and *H. chlorum* radicals and has a "turning point" line shape consistent with an $A_{||}$ component. Furthermore, it is the only nonexchangeable feature in the *H. chlorum* spectrum with an hfc that is greater than that of feature 4 and therefore able to fulfill the above relationship. Therefore, feature 6 is assigned to the 2-methyl hfc $A_{||}$ component. Note that the ~3.5 MHz difference between the $A_{||}$ and $A_\perp$ components arises from the high unpaired electron spin densities at semiquinone oxygens and is therefore diagnostic for semiquinone radicals.

Features 1 and 3 have the line shapes associated with $A_\perp$ and $A_{||}$ components, respectively, of an axial hfc. With the methyl and H-bond protons having been assigned, only features arising from the initial (1′) methylene group of the long hydrocarbon (isoprenoid) "tail" attached at C(3) and the ring protons at C(5)−C(8) remain to be assigned. Solution state spectra of phylloquinone and menadione (2-methylnaphthoquinone) (*44*) suggest that the hfcs to the ring protons are less than 2 MHz and are hidden under the central matrix feature in frozen solution spectra. Therefore, features 1 and 3 are assigned to the protons of the 1′-CH_2 group attached at C(3). Since only one axial hfc is observed in the ENDOR spectra, it is assumed that this represents equivalent coupling to both methylene protons (but see below).

Features 1, 2, and 4 do overlap somewhat in the ENDOR spectra of Figure 2. This is due to the high-rf modulation depths required to obtain ENDOR spectra with good signal to noise in reasonable time. Using lower modulation depths would improve the resolution, but would carry an unacceptable signal-to-noise penalty. This problem can be overcome in part by using electron−nuclear−nuclear special TRIPLE (ST) spectroscopy (*58*, *59*). ST spectroscopy produces a "half-ENDOR" spectrum with increased intensity, in which the hfcs can be read off as twice the frequency axis position. The increased intensity of ST spectroscopy can be used to offset the signal-to-noise decrease arising from lower modulation depths, and thus allows spectra to be obtained at a higher resolution. ST spectra of the *C. limicola* and *H. chlorum* radicals are shown in Figure 5. These spectra show clearly resolved features, including two components of feature 2 in the *H. chlorum* radical (Figure 5b). The presence of two components in feature 2 in ST spectra of *C. limicola* is demonstrated in Figure 6b (see below). Feature 1 is also more clearly separated from the other features and partially resolved into two components in the *C. limicola* spectrum (Figure 5a), suggesting inequivalence in the hfcs to the two β-CH_2 protons. Surprisingly, feature 3 in the *C. limicola*

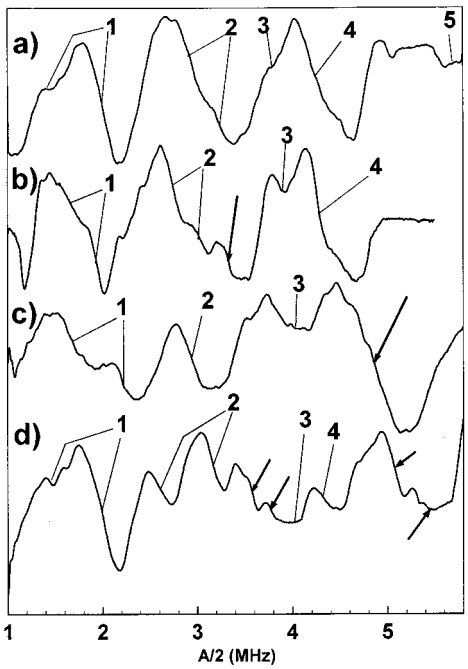

FIGURE 6: Special TRIPLE spectra of radicals photoaccumulated in *C. limicola* treated in various ways: (a) in membranes, (b) solubilized using dodecyl maltoside, (c) solubilized using Triton X-100, and (d) in a dodecyl maltoside-solubilized preparation exposed to oxygen. Conditions were like those described in the legend of Figure 5a.

spectrum is somewhat obscured in the ST spectrum (Figure 5a), apparently due to an increase in the relative intensity of feature 4. This prevents such inequivalence in the two β-CH_2 proton $A_\perp$ components of feature 1 from also being detected in the $A_{||}$ components of the same hfc that gives rise to feature 3. Feature 5 is just visible at the high-frequency edge of the ST spectra. The assignments and hfcs of the features denoted in both the ENDOR and ST spectra are collected in Table 1 and there compared with the hfcs and assignments for the $A_1^{\bullet-}$ phyllosemiquinone radical of PSI.

The successful application of ST spectroscopy to the membrane systems has enabled us to study modifications to the *C. limicola* system which produce weaker and/or more complex spectra. Treatment of the membrane preparations with *n*-dodecyl β-D-maltoside (DM) produces a solubilized reaction center preparation in which a radical can be generated by illumination for 2 min at 205 K (with dithionite). Figure 6b shows the ST spectrum of this radical. The features of this spectrum have somewhat narrower line shapes than in the ST spectrum of the radical formed in *C. limicola* membranes (Figure 5a and repeated for reference in Figure 6a), allowing for better resolution of feature 3. Although the line shapes of the features have been changed, their positions (and hence hfcs) remain very similar to those observed for the membrane sample. One new feature is observed, denoted with an arrow in Figure 6b, but the low intensity of this feature shows that it is present in only a small minority of centers. These observations suggest that the radical environment is not greatly perturbed by the DM treatment.

Treatment of membranes with Triton X-100 and subsequent illumination at 205 K for 2 min in the presence of dithionite produces the ST spectrum shown in Figure 6c. Features 1−3 are present but perturbed, with feature 1 being clearly resolved into two components (it is possible that one of these is a new feature), while feature 2 now appears as a single line and feature 3 is broader (possibly as a consequence of the change in feature 1 as both these arise from the β-CH_2 protons). Feature 4 is not evident, and a new feature (denoted with an arrow in the spectrum) occurs with an hfc of 9.8 MHz. This latter feature is rather intense and could arise from a superposition of several lines.

C. limicola is an obligate anaerobe, and its photosynthetic reaction center seems to be damaged by oxygen. Therefore, exposure of the RC to oxygen followed by radical generation and spectroscopic analysis may provide some indication as to the nature of the oxygen-induced damage. Such an experiment was performed using DM-solubilized RCs which were exposed to the air for 30 min at 4 °C, and the ST spectrum that is obtained is shown in Figure 6d. There are several noteworthy differences relative to the ST spectrum of the DM-solubilized preparation shown in Figure 6b. Feature 1 exhibits an increased intensity and a line shape change. The two components of feature 2 have apparently diverged, giving rise to two distinct hfcs. Both new feature 2 hfcs, however, lay within the line shape of feature 2 in the anaerobic DM spectrum (Figure 6b). Features 3 and 4 are present but reduced in intensity. Conversely, the unassigned minor feature of Figure 6b has increased in intensity and is now flanked to high frequency by another small unassigned feature (both denoted with arrows). A new pair of features (denoted with arrows), which apparently form a system with a small axial anisotropy (i.e., they are an $A_\perp$ and an $A_{||}$ component of the same hfc), is present around an hfc of 10 MHz. These latter features and the increased intensity of feature 1 may arise from the generation of a chlorophyll anion radical in these RCs (S. E. J. Rigby et al., unpublished observations).

DISCUSSION

The presence of an (methyl) hfc with an $A_{||} - A_\perp$ value of 3.5 MHz and two large H-bond hfcs in the spectra of both the *C. limicola* and *H. chlorum* radicals is clearly suggestive of a methyl-substituted semiquinone, albeit in an unusual environment. The data collected in Table 1 reveal a striking similarity between the hfcs arising from the *C. limicola* and *H. chlorum* radicals and the $A_1^{\bullet-}$ phyllosemiquinone radical of PSI. Both $A_1^{\bullet-}$ and the radicals studied here exhibit a semiquinone methyl hfc which is significantly increased relative to those reported for any in vitro semiquinone species, and two similar but distinct H-bond hfcs. The methyl hfcs are, however, slightly smaller (<5%) in the *C. limicola* and *H. chlorum* radicals, and there are differences between the H-bond hfcs of all three radicals. The *H. chlorum* radical in particular exhibits a 1.5 MHz difference between the two H-bond $A_\perp$ components, compared to the 0.8 MHz of the *C. limicola* radical and $A_1^{\bullet-}$. This suggests a less symmetric H-bonding environment in *H. chlorum.*

The hfcs to methylene (CH_2) protons β to the quinone ring are a function of both the spin density at the attached carbon and the angle between the C−H bond and the normal to the quinone ring plane. This is described by the Heller−McConnell relation (*60*):

$$A_{iso} = Q\rho_c \cos^2 \theta$$

where Q is a constant equal to 162 MHz, ρ_c is the unpaired electron spin density at the attached ring carbon, and θ is the angle between the C−H bond and the quinone ring normal. The observation of two distinct β-CH_2 hfcs in *C. limicola* suggests that the orientation of the quinone ring is not symmetrical relative to the two β-CH_2 protons in this radical (i.e., different θ for each proton), unlike $A_1^{\bullet-}$. The decreased but single β-CH_2 hfc in the *H. chlorum* radical suggests a decrease in the electron spin density (ρ_c) at C(3) relative to that of *C. limicola* and $A_1^{\bullet-}$, perhaps as a consequence of the different H-bond arrangement in *H. chlorum*.

The approximate hydrogen bond O−H distance may be estimated from the equation

$$A = \rho\frac{78.4}{r^3}(3\cos^2\theta - 1)$$

where A is the component of the H-bond hyperfine coupling constant, ρ is the oxygen π spin density, r is the O−H distance, and θ is the angle between the applied field and the hyperfine coupling tensor, i.e., 0° for $A_{||}$ and 90° for $A_\perp$. The value of ρ has been estimated for naphthosemiquinones in vitro (*66*) to be 0.2. Although the methyl group hfcs suggest that the electron spin density distribution is distorted in the semiquinones studied here relative to those in vitro, this value will allow for an approximate determination of the O−H distance. The O−H distances so calculated are 1.33 and 1.47 Å for *H. chlorum* and 1.36 and 1.42 Å for *C. limicola*. The distance calculated for benzosemiquinone by O'Malley and Babcock (*55*) is 1.55 Å, suggesting somewhat stronger H-bonding in the *H. chlorum* and *C. limicola* forms than is typical for semiquinones in vitro.

When the *C. limicola* RC is solubilized using *n*-dodecyl β-D-maltoside (DM), the ST spectrum of the radical exhibits altered line shapes relative to that of the membrane sample, but essentially the same hfcs. Only the hfcs to the β-CH_2 protons are affected, possibly due to a slight reorientation of the quinone ring. The line shape differences suggest changes in the dynamics of the quinone binding site, leading to differences in nuclear relaxation. Therefore, DM is capable of solubilizing the *C. limicola* RC with the quinone binding site essentially intact. Kjaer et al. (*61*) also used anaerobic conditions and *n*-dodecyl β-D-maltoside to solubilize reaction centers from *Chlorobium vibrioforme* that contained 1.7 menaquinones per reaction center.

Treatment with Triton X-100 on the other hand leads to the loss of the methyl group feature (feature 4). Furthermore, only one H-bond feature is observed, indicating changes in semiquinone−protein interactions. Such effects of Triton X-100 were also reported in our previous study of $A_1^{\bullet-}$ (*45*). However, here the β-CH_2 features are also affected, and new features arise in the spectrum which are not obviously related to the semiquinone. These new features presumably arise from some other radical species (probably a chlorophyll anion; see below) which is photoaccumulated in reaction centers where the quinone site is damaged by the Triton treatment. Interestingly, Triton X-100 has been shown to remove phylloquinone in photosystem I preparations that lack the iron−sulfur centers (*62*).

C. limicola and *H. chlorum* are obligate anaerobes, and we take great care to exclude oxygen in the preparation of samples. We believe that oxygen can damage the photosynthetic reaction centers in these organisms, although the site of oxygen damage in the RC is not known. Spectroscopic examination of DM-solubilized RCs which have been exposed to oxygen may help to locate this site. The results of such an experiment reported here show that oxygen affects the environment of the bound quinone in *C. limicola*. Moreover, a new radical species is formed in many RCs that appears be a chlorophyll (not a bacteriochlorophyll) anion radical (S. E. J. Rigby et al., manuscript in preparation). This may be analogous to the situation where the primary acceptor $A_0^{\bullet-}$ radical is photoaccumulated in PSI when the phylloquinone is either doubly reduced or removed (*51*). Oxygen does not affect the phylloquinone binding pocket in PSI, but it is possible that the site of oxygen damage in the reaction center of *C. limicola* is the F_X center. Damage to F_X is known to affect the stability of phylloquinone in PSI (*62*).

It is clear from the results presented above that the reaction centers of green sulfur bacteria and heliobacteria contain a semiquinone electron acceptor that can be photoaccumulated at 205 K in the same way as phyllosemiquinone in PSI. The ENDOR spectra suggest a menaquinone, and indeed, menaquinone is the only quinone present in heliobacteria (*22*). Given the appearance of β-CH_2 methylene protons, the ENDOR spectra are unlikely to arise from the quinones other than menaquinone found in green sulfur bacteria [oxomenaquinone (*Chlorobium* quinone) or 1′-hydroxymenaquinone]. The conclusion that the signals arise from menasemiquinone is in agreement with the recent report of 1.7 menaquinones being associated with reaction center preparations from *C. vibrioforme* (*61*). Dark reduction with sodium dithionite or photoaccumulation at 205 K produced an asymmetric EPR signal in these preparations whose spectrum at 34 GHz was said to be consistent with its identification as arising from a combination of a menasemiquinone and a (bacterio)chlorophyll anion (although it may arise from a combination of a menasemiquinone and $P840^{+\bullet}$). We only observe photoaccumulation of a menasemiquinone. This difference may be a consequence of the photoaccumulation procedure used by Kjaer et al. (*61*) which was carried out at pH 10 (see ref *51*), damage to some of the reaction centers in the preparations used by Kjaer et al. (*61*), or differences between *C. vibrioforme* and the organisms we studied.

Although there is a different H-bonding arrangement (perhaps less symmetric) to the semiquinone in *H. chlorum*, it is striking how similar the electronic structure of semiquinones in these reaction centers is to that of the phyllosemiquinone in PSI. This suggests that the binding pocket for the semiquinones is conserved, and that the same mechanism may be used in all type I reaction centers to modify the operating redox potential of the quinone/semiquinone redox couple to enable it to function at low redox potentials.

There is no conclusive evidence as yet that the semiquinone in the reaction centers of green sulfur bacteria and heliobacteria is kinetically competent to function in, or necessary for, forward electron transfer from A_o to F_X in these reaction centers. However, it is arguable that forward electron transfer from A_o to F_X could account for the observed rates of 600 ps for forward electron transfer from A_o (*31*−*33*). The conservation of the F_X binding sequence and the histidine residues on the electron donor side of the

reaction centers of green sulfur bacteria and heliobacteria compared to PSI suggests that the center−center distance between F_X and A_o in green sulfur bacteria and heliobacteria is the same as the 20 or 22 Å reported for PSI (*63*). If one assumes that electron transfer is optimized ($-\Delta G^\circ = \lambda$), then the electron transfer rate can be calculated from the distance alone using the simplified form of the equation taken from Moser and Dutton (*64*).

$$\log k_{et} = 15 - 0.6R$$

The distance relevant is the edge-to-edge distance which is probably no less than 12 Å (allowing an effective distance of 6 Å from the center of the chlorophyll A_o to the edge and 2 Å for F_X). This would predict a rate for forward electron transfer from A_o to F_X of around 4 ns, whereas a rate of 600 ps is reported for the reoxidation of A_o^- by forward electron transfer (*31*−*33*). Therefore, the 600 ps reoxidation of A_o^- is unlikely to reflect electron transfer to F_X but could reflect electron transfer to a quinone. Electron transfer from A_o^- to the PhQ A_1 in PSI takes between 20 and 30 ps (*34*−*36*). However, if the menaquinone in these type I bacterial reaction centers was further away from A_o than the phylloquinone is from A_o in PSI, the time constant for reoxidation of A_o could increase from 20−30 to 600 ps. The photovoltaic measurements of Brettel et al. (*38*) suggest that the distance from A_o to the next acceptor on this 600 ps time scale in bacterial type I RCs is equivalent to the distance from A_o to F_X in PSI. If the quinone in the homodimeric reaction centers was in the same position as the quinone bound to the reaction centers of purple bacteria, then the distance from A_o to MQ would be similar to the A_o to F_X distance in PSI (*38*), and a longer time for electron transfer from A_o^- to MQ than the 20−30 ps observed for transfer from A_o^- to A_1 in PSI is expected. The suggestion that the time needed for forward transfer from A_o^- to MQ in bacterial type I RCs is 600 ps compared to the value of 200 ps observed for bacteriopheophytin to ubiquinone in the RCs of purple bacteria could be explained by the difference in the driving force. However, if there is only a small difference between the rate of electron transfer from A_o to F_X (4 ns) or A_1 (600 ps), then the menaquinone might not be an obligate component of forward electron transfer in bacterial type I reaction centers.

ACKNOWLEDGMENT

We thank A. H. M. de Wit, H. Leech, and P. Ratnesar for technical assistance.

REFERENCES

1. Sakurai, H., Kusumoto, N., and Inoue, K. (1996) *Photochem. Photobiol. 64*, 5−13.
2. Olson, J. M. (1998) *Photochem. Photobiol. 67*, 61−75.
3. Lockau, W., and Nitschke, W. (1993) *Physiol. Plant. 88*, 372−381.
4. Amesz, J. (1995) in *Anoxygenic Photosynthetic Bacteria* (Blankenship, R. E., Madigan, M. T., and Bauer, C. E., Eds.) pp 687−697, Kluwer Academic Publishers, Dordrecht, The Netherlands.
5. Feiler, U., and Hauska, G. (1995) in *Anoxygenic Photosynthetic Bacteria* (Blankenship, R. E., Madigan, M. T., and Bauer, C. E., Eds.) pp 665−685, Kluwer Academic Publishers, Dordrecht, The Netherlands.
6. Olson, J. M. (1996) *Photochem. Photobiol. 64*, 1−4.
7. Blankenship, R. E. (1992) *Photosynth. Res. 33*, 91−111.
8. Rigby, S. E. J., Thapar, R., Evans, M. C. W., and Heathcote, P. (1994) *FEBS Lett. 350*, 24−28.
9. Feiler, U., Albouy, D., Robert, B., and Mattioli, T. A. (1995) *Biochemistry 34*, 11099−11105.
10. Van de Meent, E. J., Kobayashi, M., Erkelens, C., van Veelen, P. A., Amesz, J., and Watanabe, T. (1991) *Biochim. Biophys. Acta 1058*, 356−362.
11. Feiler, U., Albouy, D., Pourret, C., Mattioli, T. A., Lutz, M., and Robert, B. (1994) *Biochemistry 33*, 7594−7599.
12. Büttner, M., Xie, D. L., Welson, H., Pinther, W., Hauska, G., and Nelson, N. (1992) *Proc. Natl. Acad. Sci. U.S.A. 89*, 8135−8139.
13. Illinger, N., Xie, D.-L., Hauska, G., and Nelson, N. (1993) *Photosynth. Res. 38*, 111−114.
14. Nitschke, W., Feiler, U., and Rutherford, A. W. (1990) *Biochemistry 29*, 3834−3842.
15. Nitschke, W., Sétif, P., Liebl, U., Feiler, U., and Rutherford, A. W. (1990) *Biochemistry 29*, 11079−11088.
16. Liebl, U., Mockensturm-Wilson, M., Trost, J. T., Brune, D. C., Blankenship, R. E., and Vermaas, W. (1993) *Proc. Natl. Acad. Sci. U.S.A. 90*, 7124−7128.
17. Büttner, M., Xie, D. L., Nelson, H., Pinther, W., Hauska, G., and Nelson, N. (1992) *Biochim. Biophys. Acta 1101*, 154−156.
18. Moenne-Loccoz, P., Heathcote, P., MacLachlan, D. J., Berry, M. C., Davis, I. H., and Evans, M. C. W. (1994) *Biochemistry 33*, 10037−10042.
19. Van der Est, A., Bock, C., Golbeck, J., Brettel, K., Setif, P., and Stehlik, D. (1994) *Biochemistry 33*, 11789−11797.
20. Luneberg, J., Fromme, P., Jekow, P., and Schlodder, E. (1994) *FEBS Lett. 203*, 225−229.
21. Brettel, K. (1997) *Biochim. Biophys. Acta 1318*, 322−373.
22. Hiraishi, A. (1989) *Arch. Microbiol. 151*, 378−379.
23. Powls, R., and Redfearn, E. R. (1969) *Biochim. Biophys. Acta 172*, 429−437.
24. Brok, M., Vasmel, H., Horikx, J. T. G., and Hoff, A. J. (1986) *FEBS Lett. 194*, 322−326.
25. Nitschke, W., Feiler, U., Lockau, W., and Hauska, G. (1987) *FEBS Lett. 218*, 283−286.
26. Chiou, H.-C., and Blankenship, R. E. (1996) *Photochem. Photobiol. 64*, 32−37.
27. Trost, J. T., Brune, D. C., and Blankenship, R. E. (1992) *Photosynth. Res. 32*, 11−22.
28. Kleinherenbrink, F. A. M., Ikegami, I., Hiraishi, A., Otte, S. C. M., and Amesz, J. (1993) *Biochim. Biophys. Acta 1142*, 69−73.
29. Frankenberg, N., Hager-Braun, C., Feiler, U., Fuhrmann, M., Rogl, H., Schneebauer, N., Nelson, N., and Hauska, G. (1996) *Photochem. Photobiol. 64*, 14−19.
30. Miller, M., et al. (1998) *Photosynthesis Congress* (in press).
31. Nuijs, A. M., Vasmel, H., Joppe, H. L. P., Duysens, L. N. M., and Amesz, J. (1985) *Biochim. Biophys. Acta 807*, 24−34.
32. Nuijs, A. M., van Dorssen, R. J., Duysens, L. N. M., and Amesz, J. (1985) *Proc. Natl. Acad. Sci. U.S.A. 82*, 6865−6868.
33. Lin, S., Chiou, H.-C., Kleinherenbrink, F. A. M., and Blankenship, R. E. (1994) *Biophys. J. 66*, 437−445.
34. Hastings, G., Kleinherenbrink, F. A. M., Lin, S., McHugh, T. J., and Blankenship, R. E. (1994) *Biochemistry 33*, 3193−3200.
35. Kumazaki, S., Iwaki, M., Ikegami, I., Kandori, H., Yoshihara, K., and Itoh, S. (1994) *J. Phys. Chem. 98*, 11220−11225.
36. White, N. T. H., Beddard, G. S., Thorne, J. R. G., Feehan, T., Keyes, T. E., and Heathcote, P. (1996) *J. Phys. Chem. 100*, 12086−12099.
37. Lin, S., Chiou, H.-C., and Blankenship, R. E. (1995) *Biochemistry 34*, 12761−12767.
38. Brettel, K., Liebl, W., and Liebl, U. (1998) *Biochim. Biophys. Acta 1363*, 175−181.
39. Heathcote, P., and Warden, J. T. (1982) *FEBS Lett. 140*, 277−281.

40. Snyder, S. W., and Thurnauer, M. C. (1993) in *The Photosynthetic Reaction Center* (Norris, J. R., and Deisenhofer, J., Eds.) Vol. II, Chapter 11, Academic Press, New York.
41. Bonnerjea, J., and Evans, M. C. W. (1982) *FEBS Lett. 148*, 313−316.
42. Gast, P., Swarthoff, T., Ebskamp, F. C. R., and Hoff, A. J. (1983) *Biochim. Biophys. Acta 722*, 163−175.
43. Heathcote, P., Moenne-Loccoz, P., Rigby, S. E. J., and Evans, M. C. W. (1996) *Biochemistry 35*, 6644−6650.
44. Barry, B. A., Bender, C. J., McIntosh, L., Ferguson-Miller, S., and Babcock, G. T. (1988) *Isr. J. Chem. 28*, 129−132.
45. Rigby, S. E. J., Evans, M. C. W., and Heathcote, P. (1996) *Biochemistry 35*, 6651−6656.
46. Muhiuddin, I. P., Rigby, S. E. J., Evans, M. C. W., and Heathcote, P. (1995) in *Photosynthesis: from Light to Biosphere* (Mathis, P., Ed.) Vol. II, pp 159−162, Kluwer Academic Publishers, Dordrecht, The Netherlands.
47. Bratt, P. J., Muhiuddin, I. P., Evans, M. C. W., and Heathcote, P. (1996) *Photochem. Photobiol. 64*, 20−25.
48. Van de Meent, E. J., Kleinherenbrink, F. A. M., and Amesz, J. (1990) *Biochim. Biophys. Acta 1015*, 223−230.
49. Hager-Braun, C., Xie, D.-L., Jarosch, U., Herold, E., Buttner, M., Zimmerman, R., Deutzmann, R., Hauska, G., and Nelson, N. (1995) *Biochemistry 34*, 9617−9624.
50. Feiler, U., Nitschke, W., and Michel, H. (1992) *Biochemistry 31*, 2608−2614.
51. Heathcote, P., Hanley, J. A., and Evans, M. C. W. (1993) *Biochim. Biophys. Acta 1144*, 54−61.
52. Rigby, S. E. J., Nugent, J. H. A., and O'Malley, P. J. (1994) *Biochemistry 33*, 1734−1742.
53. Rigby, S. E. J., Nugent, J. H. A., and O'Malley, P. J. (1994) *Biochemistry 33*, 10043−10050.
54. O'Malley, P. J., and Babcock, G. T. (1986) *J. Am. Chem. Soc. 108*, 3995−4001.
55. O'Malley, P. J., and Babcock, G. T. (1984) *J. Chem. Phys. 80*, 3912−3913.
56. Hoganson, C. W., and Babcock, G. T. (1992) *Biochemistry 31*, 11874−11880.
57. Zheng, M., and Dismukes, G. C. (1996) *Biochemistry 35*, 8955−8963.
58. Freed, J. H. (1969) *J. Chem. Phys. 50*, 2271.
59. Dinse, K. P., Biehl, R., and Möbius, K. (1974) *J. Chem. Phys. 61*, 4335.
60. Heller, H. C., and McConnell, H. M. (1960) *J. Chem. Phys. 32*, 1535.
61. Kjaer, B., Frigaard, N.-U., Yang, F., Zybailov, B., Miller, M., Golbeck, J. H., and Scheller, H. V. (1998) *Biochemistry 37*, 3237−3242.
62. Warren, P. V., Golbeck, J. H., and Warden, J. T. (1993) *Biochemistry 32*, 849−857.
63. Krauss, N., Schubert, W.-D., Klukas, O., Fromme, P., Witt, H. T., and Saenger, W. (1996) *Nat. Struct. Biol. 3*, 965−973.
64. Moser, C. C., and Dutton, P. L. (1992) *Biochim. Biophys. Acta 1101*, 171−176.
65. Van de Meent, E. J., Koayashi, M., Erkelens, C., van Veelen, P. A., Otte, S. C. M., Inoue, K., Watanabe, T., and Amesz, J. (1992) *Biochim. Biophys. Acta 1102*, 371−378.
66. Hanley, J., Deligiannakis, Y., MacMillan, F., Bottin, H., and Rutherford, A. W. (1997) *Biochemistry 36*, 11543−11549.
67. Allen, J. P., and Feher, G. (1984) *Proc. Natl. Acad. Sci. U.S.A. 81*, 4795−4799.

BI982042U